Supplement of Ocean Sci., 20, 835–885, 2024
https://doi.org/10.5194/os-20-835-2024-supplement
© Author(s) 2024. CC BY 4.0 License.

Ocean Science
Open Access

Supplement of

Twenty-first century marine climate projections for the NW European shelf seas based on a perturbed parameter ensemble

Jonathan Tinker et al.

Correspondence to: Jonathan Tinker (jonathan.tinker@metoffice.gov.uk)

The copyright of individual parts of the supplement might differ from the article licence.

Supplement

S1.1 Additional Tables

Table S1 Temperature and Salinity biases when comparing the ensemble mean NWSPPE to the ICES long term climate *in situ* observation timeseries. The mean absolute bias is the ensemble and temporal NWSPPE mean minus the observations mean, the relative mean bias is the absolute bias divided by the ensemble standard deviations giving the number of ensemble standard deviations the observations are from the NWSPPE ensemble mean. The Relative Interannual Variability Bias is the ratio of the observations interannual variability to the mean of the interannual variability of all the ensemble members.

	Temperature Bias			Salinity Bias		
	Absolute Mean Bias	**Relative Mean Bias**	**Relative Interannual Variability Bias**	**Absolute Mean Bias**	**Relative Mean Bias**	**Relative Interannual Variability Bias**
Faroe Shetland NAW	-1.10	-3.02	2.88	0.02	0.23	1.61
Faroe Shetland MNAW	-1.01	-2.91	1.18	0.06	0.68	0.44
Utsira A	-0.42	-1.37	-1.97	0.22	3.24	-1.95
Utsira B	-0.97	-3.72	-2.38	0.11	1.67	-1.25
Fair Isle Current Water	-0.83	-2.69	1.79	0.42	5.98	-0.89
Helgoland Roads	-0.56	-1.11	0.99	-0.71	-3.58	-3.05
Plymouth WCO E1	-0.09	-0.32	-4.89	0.19	1.91	0.75
Astan	0.04	0.11	0.63	0.28	3.08	-1.90
Irish Sea AFBI	-0.10	-0.29	-1.51			
Ireland M3	0.50	1.67	0.94			
Ireland Malin	0.38	1.26	1.27			

Table S2 Volume tranport through cross-sections. Section names, with associate figures (Figure S7-S14), early and late century ensmeble mean net transport, and the percentage change, with the latitude and longitude of transect ends.

Section name	**Figure**	**Ens Mean (2000-2019)**	**Ens Mean (2079-2098)**	**% increase over 21st Century**	**Start point**	**End Point**
54 Slope current 48.2N	Figure S7a	0.390	1.729	343.8%	47.93°N 9.44°W	48.47°N 9.00°W
56 Slope current 53.9N	Figure S7b	0.508	1.418	179.0%	54.07°N 12.78°W	53.67°N 12.78°W
58 Slope current 54.8N	Figure S7c	1.195	0.320	-73.2%	54.93°N 10.44°W	54.60°N 10.11°W
59 Slope current 57.0N	Figure S8a	1.299	0.416	-68.0%	56.93°N 9.33°W	57.13°N 9.00°W
60 Slope current 58.4N	Figure S8b	2.163	1.919	-11.3%	58.60°N 9.22°W	58.27°N 9.00°W
61 Slope current 58.7N	Figure S8c	2.795	1.090	-61.0%	59.00°N 8.00°W	58.47°N 7.33°W
65 Slope current 62.0N	Figure S9a	2.187	5.509	151.9%	62.27°N 0.22°E	61.80°N 0.22°E
66 Slope current 62.7N	Figure S9b	2.759	3.759	36.3%	63.00°N 4.00°E	62.40°N 4.22°E
67 Slope current 63.2N	Figure S9c	2.908	3.632	24.9%	63.47°N 5.11°E	62.93°N 5.56°E
85 NNSI BA	Figure S10a	2.921	9.269	217.4%	62.93°N 1.22°E	61.20°N 1.22°E
86 NNSI CA	Figure S10b	0.944	1.306	38.3%	61.87°N 2.33°E	61.20°N 1.22°E
87 NNSI BC	Figure S10c	1.977	7.963	302.8%	62.93°N 1.22°E	61.87°N 2.33°E
89 NNSI DC	Figure S11a	2.021	7.804	286.1%	63.13°N 2.33°E	61.87°N 2.33°E
90 NNSI DE	Figure S11b	3.684	9.570	159.8%	63.13°N 2.33°E	62.33°N 4.22°E
91 NNSI CE	Figure S11c	1.662	1.766	6.2%	61.87°N 2.33°E	62.33°N 4.22°E
45 Scotland Orkney	Figure S12a	0.092	0.078	-15.3%	58.67°N 3.22°W	59.20°N 2.78°W
46 Orkney FairIsle	Figure S12b	0.307	0.182	-40.6%	59.20°N 2.67°W	60.07°N 1.33°W
47 Shetland N	Figure S12c	0.394	0.449	14.0%	60.73°N 0.78°W	60.73°N 3.00°E

34 Dover Strait	Figure S13a	0.072	0.041	-43.7%	51.13°N 1.44°E	50.93°N 1.78°E
33 Noordwijk	Figure S13b	0.075	0.043	-42.6%	52.47°N 1.78°E	52.47°N 4.56°E
36 Dublin-Holyhead	Figure S13c	0.019	-0.025	-227.9%	53.40°N 6.00°W	53.40°N 4.56°W
98 UKCP09 03 Dooley Current	Figure S14a	0.256	0.202	-21.2%	58.00°N 0.00°W	57.00°N 0.00°W
44 NSea Skag (out of Baltic)	Figure S14b	1.220	1.013	-17.0%	57.20°N 9.00°E	58.47°N 9.00°E
44 NSea Skag (into Baltic)	Figure S14c	1.218	1.011	-17.0%	57.20°N 9.00°E	58.47°N 9.00°E

Table S3 MLD for summer and autumn. Note the grid boxes where the PEA < 20 J/m^3 have been masked out prior to calculation of the regional statistics. Ensemble mean changes are given with ±2 (ensemble) standard deviations.

MLD	Shelf	Southern North Sea	Central North Sea	Northern North Sea	English Channel	Irish Sea	Celtic Sea
JJA	-3.33 m (±2.17 m)	-2.78 m (±1.65 m)	-2.17 m (±1.55 m)	-2.01 m (±2.01 m)	-4.13 m (±2.67 m)	-6.03 m (±3.57 m)	-3.00 m (±1.40 m)
SON	-12.30 m (±6.69 m)	-0.11 m (±0.86 m)	-7.19 m (±3.82 m)	-8.23 m (±6.26 m)	0.31 m (±0.24 m)	-9.39 m (±8.65 m)	-9.55 m (±4.50 m)

Table S4 Projected regional mean Potential Energy Anomaly (PEA) changes between 2000-2019 and 2079-2098. 10 J/m^3 is considered the threshold for stratification. Ensemble mean changes are given with ±2 (ensemble) standard deviations.

PEA	Shelf	Southern North Sea	Central North Sea	Northern North Sea	English Channel	Irish Sea	Celtic Sea
ANN	17.41 J/m^3 (±13.40 J/m^3)	0.57 J/m^3 (±0.63 J/m^3)	10.02 J/m^3 (±4.49 J/m^3)	14.87 J/m^3 (±13.50 J/m^3)	1.75 J/m^3 (±0.81 J/m^3)	3.89 J/m^3 (±2.18 J/m^3)	36.25 J/m^3 (±25.67 J/m^3)
DJF	8.52 J/m^3 (±9.99 J/m^3)	-0.17 J/m^3 (±0.42 J/m^3)	0.02 J/m^3 (±0.44 J/m^3)	4.25 J/m^3 (±9.01 J/m^3)	-0.03 J/m^3 (±0.18 J/m^3)	-0.08 J/m^3 (±0.98 J/m^3)	27.87 J/m^3 (±23.69 J/m^3)
MAM	4.06 J/m^3 (±8.53 J/m^3)	0.22 J/m^3 (±0.97 J/m^3)	1.69 J/m^3 (±2.56 J/m^3)	3.49 J/m^3 (±8.66 J/m^3)	0.40 J/m^3 (±0.48 J/m^3)	1.33 J/m^3 (±1.96 J/m^3)	10.53 J/m^3 (±17.87 J/m^3)
JJA	24.03 J/m^3 (±17.14 J/m^3)	2.03 J/m^3 (±1.55 J/m^3)	21.57 J/m^3 (±8.78 J/m^3)	22.71 J/m^3 (±18.74 J/m^3)	4.03 J/m^3 (±1.58 J/m^3)	10.11 J/m^3 (±4.56 J/m^3)	41.12 J/m^3 (±28.00 J/m^3)
SON	32.84 J/m^3 (±21.40 J/m^3)	0.22 J/m^3 (±0.50 J/m^3)	16.77 J/m^3 (±8.91 J/m^3)	28.98 J/m^3 (±23.80 J/m^3)	2.60 J/m^3 (±1.44 J/m^3)	4.21 J/m^3 (±3.02 J/m^3)	64.99 J/m^3 (±37.43 J/m^3)

Table S5 Projected regional mean Potential Energy Anomaly (temperature component, PEAT) changes between 2000-2019 and 2079-2098. 10 J/m^3 is considered the threshold for stratification. Ensemble mean changes are given with ±2 (ensemble) standard deviations.

PEAT	**Shelf**	**Southern North Sea**	**Central North Sea**	**Northern North Sea**	**English Channel**	**Irish Sea**	**Celtic Sea**
ANN	9.81 J/m^3 (±5.80 J/m^3)	0.44 J/m^3 (±0.25 J/m^3)	10.44 J/m^3 (±3.67 J/m^3)	15.80 J/m^3 (±5.89 J/m^3)	1.87 J/m^3 (±0.71 J/m^3)	3.37 J/m^3 (±1.45 J/m^3)	14.88 J/m^3 (±9.48 J/m^3)
DJF	-0.36 J/m^3 (±4.01 J/m^3)	0.00 J/m^3 (±0.05 J/m^3)	0.20 J/m^3 (±0.25 J/m^3)	2.28 J/m^3 (±3.05 J/m^3)	-0.00 J/m^3 (±0.05 J/m^3)	0.08 J/m^3 (±0.30 J/m^3)	1.30 J/m^3 (±7.15 J/m^3)
MAM	-0.85 J/m^3 (±5.26 J/m^3)	0.17 J/m^3 (±0.15 J/m^3)	2.06 J/m^3 (±1.62 J/m^3)	2.21 J/m^3 (±3.65 J/m^3)	0.40 J/m^3 (±0.31 J/m^3)	1.02 J/m^3 (±0.74 J/m^3)	-3.71 J/m^3 (±10.18 J/m^3)
JJA	17.36 J/m^3 (±8.34 J/m^3)	1.47 J/m^3 (±0.80 J/m^3)	21.84 J/m^3 (±6.95 J/m^3)	25.97 J/m^3 (±8.84 J/m^3)	4.28 J/m^3 (±1.42 J/m^3)	8.97 J/m^3 (±3.49 J/m^3)	22.45 J/m^3 (±11.74 J/m^3)
SON	23.06 J/m^3 (±10.25 J/m^3)	0.13 J/m^3 (±0.17 J/m^3)	17.63 J/m^3 (±7.64 J/m^3)	32.65 J/m^3 (±13.47 J/m^3)	2.82 J/m^3 (±1.41 J/m^3)	3.39 J/m^3 (±2.17 J/m^3)	39.45 J/m^3 (±14.86 J/m^3)

Table S6 Projected regional mean Potential Energy Anomaly (salinity component, PEAS) changes between 2000-2019 and 2079-2098. 10 J/m^3 is considered the threshold for stratification. Ensemble mean changes are given with ±2 (ensemble) standard deviations.

PEAS	Shelf	Southern North Sea	Central North Sea	Northern North Sea	English Channel	Irish Sea	Celtic Sea
ANN	7.60 J/m^3 (±13.53 J/m^3)	0.13 J/m^3 (±0.44 J/m^3)	-0.42 J/m^3 (±1.86 J/m^3)	-0.92 J/m^3 (±10.67 J/m^3)	-0.12 J/m^3 (±0.19 J/m^3)	0.52 J/m^3 (±1.29 J/m^3)	21.37 J/m^3 (±28.61 J/m^3)
DJF	8.87 J/m^3 (±12.61 J/m^3)	-0.17 J/m^3 (±0.46 J/m^3)	-0.18 J/m^3 (±0.41 J/m^3)	1.97 J/m^3 (±8.82 J/m^3)	-0.03 J/m^3 (±0.18 J/m^3)	-0.15 J/m^3 (±1.20 J/m^3)	26.57 J/m^3 (±28.34 J/m^3)
MAM	4.91 J/m^3 (±11.80 J/m^3)	0.05 J/m^3 (±0.86 J/m^3)	-0.37 J/m^3 (±1.48 J/m^3)	1.29 J/m^3 (±9.67 J/m^3)	0.00 J/m^3 (±0.26 J/m^3)	0.31 J/m^3 (±1.49 J/m^3)	14.24 J/m^3 (±25.19 J/m^3)
JJA	6.68 J/m^3 (±15.98 J/m^3)	0.56 J/m^3 (±0.88 J/m^3)	-0.27 J/m^3 (±3.97 J/m^3)	-3.26 J/m^3 (±14.69 J/m^3)	-0.25 J/m^3 (±0.34 J/m^3)	1.13 J/m^3 (±1.89 J/m^3)	18.67 J/m^3 (±29.97 J/m^3)
SON	9.78 J/m^3 (±16.19 J/m^3)	0.09 J/m^3 (±0.42 J/m^3)	-0.86 J/m^3 (±3.17 J/m^3)	-3.67 J/m^3 (±14.30 J/m^3)	-0.22 J/m^3 (±0.19 J/m^3)	0.81 J/m^3 (±1.85 J/m^3)	25.54 J/m^3 (±34.15 J/m^3)

Table S7 Projected regional mean DFS changes between 2000-2019 and 2079-2098. Salinities are given on the (unitless) practical salinity scale. Ensemble mean changes are given with ±2 (ensemble) standard deviations.

DFS	Shelf	Southern North Sea	Central North Sea	Northern North Sea	English Channel	Irish Sea	Celtic Sea
ANN	-0.06 (±0.15)	-0.01 (±0.03)	0.01 (±0.05)	0.02 (±0.15)	0.00 (±0.01)	-0.01 (±0.03)	-0.16 (±0.25)
DJF	-0.07 (±0.13)	0.02 (±0.03)	0.01 (±0.01)	-0.00 (±0.10)	0.00 (±0.01)	0.01 (±0.02)	-0.22 (±0.24)
MAM	-0.04 (±0.13)	-0.00 (±0.05)	0.01 (±0.04)	0.00 (±0.14)	-0.00 (±0.02)	-0.01 (±0.03)	-0.12 (±0.22)
JJA	-0.05 (±0.21)	-0.04 (±0.05)	0.00 (±0.11)	0.06 (±0.28)	0.01 (±0.01)	-0.02 (±0.05)	-0.12 (±0.28)
SON	-0.08 (±0.18)	-0.01 (±0.03)	0.02 (±0.07)	0.04 (±0.19)	0.01 (±0.01)	-0.02 (±0.03)	-0.20 (±0.32)

Table S8 Projected regional mean NBS changes between 2000-2019 and 2079-2098. Salinities are given on the (unitless) practical salinity scale. Ensemble mean changes are given with ±2 (ensemble) standard deviations.

NBS	Shelf	Southern North Sea	Central North Sea	Northern North Sea	English Channel	Irish Sea	Celtic Sea
ANN	-0.95 (±0.82)	-0.93 (±1.00)	-0.98 (±0.92)	-1.08 (±0.96)	-0.82 (±0.80)	-0.97 (±0.76)	-0.80 (±0.58)
DJF	-0.93 (±0.82)	-0.92 (±1.01)	-0.96 (±0.91)	-1.05 (±0.95)	-0.80 (±0.78)	-0.97 (±0.78)	-0.76 (±0.58)
MAM	-0.98 (±0.83)	-0.94 (±1.01)	-1.00 (±0.92)	-1.09 (±0.95)	-0.83 (±0.78)	-1.01 (±0.78)	-0.85 (±0.61)
JJA	-0.95 (±0.82)	-0.92 (±1.01)	-0.97 (±0.92)	-1.08 (±0.95)	-0.82 (±0.81)	-0.98 (±0.77)	-0.82 (±0.59)
SON	-0.93 (±0.82)	-0.93 (±1.00)	-0.97 (±0.92)	-1.09 (±0.97)	-0.81 (±0.82)	-0.90 (±0.75)	-0.78 (±0.57)

Table S9 Change in AMOC between 2000-2019 and 2079-2098.

Ensemble member	Early century (2000-2019) AMOC.	Late century (2079-2098) AMOC.	Change in AMOC between early century (2000-2019) and late century (2079-2098)
r001i1p00000	13.876	6.647	-7.229
r001i1p00605	16.888	7.965	-8.923
r001i1p00834	18.039	7.933	-10.106
r001i1p01113	13.147	6.708	-6.439
r001i1p01554	15.008	6.541	-8.466
r001i1p01649	16.892	8.825	-8.067
r001i1p01843	17.646	8.165	-9.481
r001i1p01935	17.909	10.578	-7.331
r001i1p02123	17.814	8.235	-9.579
r001i1p02242	17.259	8.666	-8.593
r001i1p02491	16.752	7.145	-9.607
r001i1p02868	13.445	6.644	-6.800

S1.2 Additional Figures

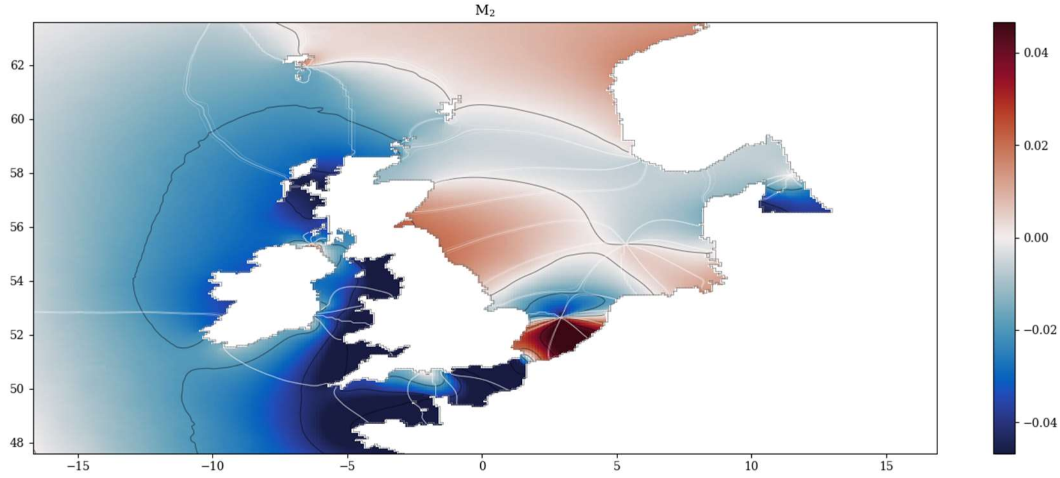

Figure S1 The impact of the Tide Generating Potential on the M_2 co-tidal chart. The difference between the tidal harmonic analysis of the simulation with the Tide Generating Potential and the unperturbed member of the PPE, the equivalent simulation with the Tide Generating Potential off. The amplitude (m) is shown with colour map (and black contours which match the tick labels of the colourbar). The phase every 45° is shown as fine white contours, for the two simulations, and the average phase of the two simulations is a bolder white line. Comparing with Figure 1a, suggests a difference of the order of 2%.

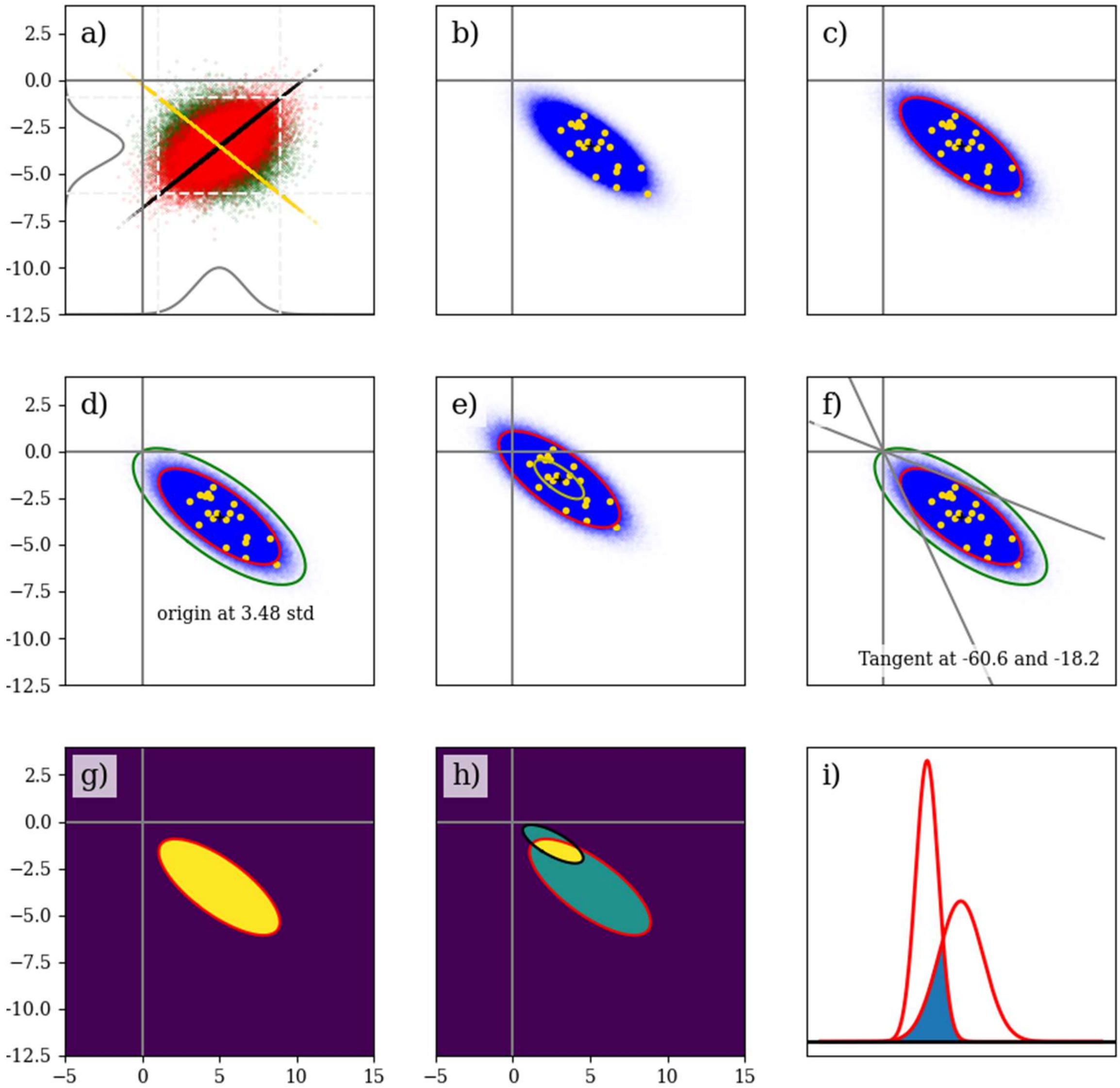

Figure S2 Reproduced from Tinker et al. (2022) to explain the residual current uncertainty ellipses method. See their additional materials for a detailed explanation. A) A bivariate normal distribution can be circular, elliptical or a straight line. b, c) when fitting an ellipse around the mean, representing 2.45 standard deviations, you capture 95% of the data, or ~19 out of 20 points. The ellipse will either d) exclude the origin, or e) include the origin, which gives a measure of how consistent, or significant, the residual current is – if it excludes the origin, you can quantify the angular width of the ellipse. Using the fitted bivariate normal distribution, and ellipse (g), you can quantify how similar two residual current distributions are, but the proportion of their overlap (h), or the volume under the Gaussian surfaces, as illustrated in 2 dimension in i – as the volume/area under a Gaussian distribution equals 1, this overlap is between ≈0 and 1. In this paper, we extend this method to give the ensemble overlap, where we find the minimum volume under all the Gaussian surfaces of the ensemble (also between ≈0 and 1).

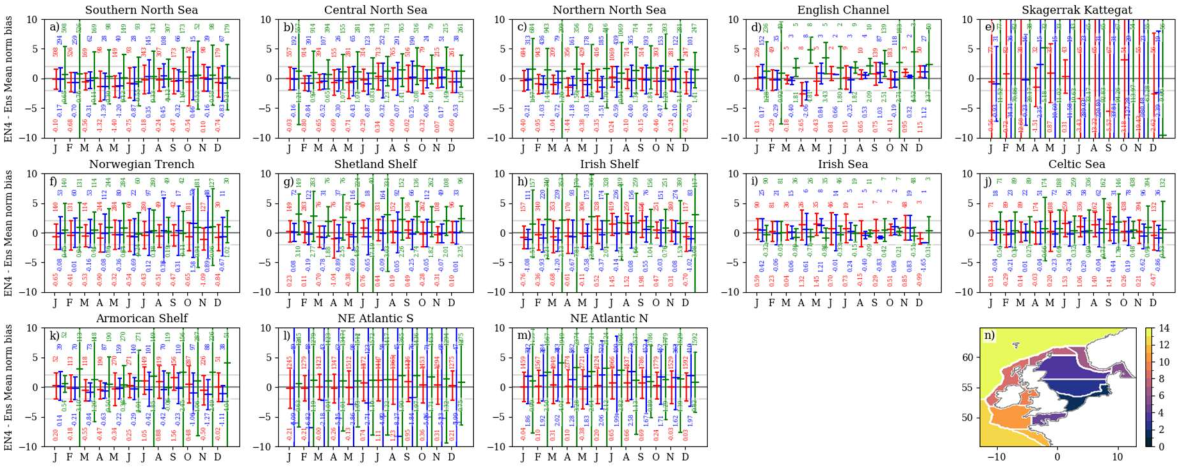

Figure S3 Regional mean distribution of normalised Model minus EN4 profile observations, for SST (red), NBT (blue) and SSS (green). Each EN4 profile – model pair is used to calculate a normalised bias (model minus ensemble mean divided by ensemble standard deviation), as shown in Figure S3-5. These data points are separated into distributions by validation regions and month – the different regions are plotted as separate subpanels, and the months are separated along the x axis (showing month number). Each distribution is plotted as the mean and ± 2 standard deviation, with 2 numbers– the number of points in each distrbution is the upper number, and the distirbution mean is the lower number. The region mask is giving in subpanel n. This figure repeats Figure 3 in the main body of the manuscript, but with the Wakelin region mask in Figure S2, giving greater granularity, but smaller sample sizes.

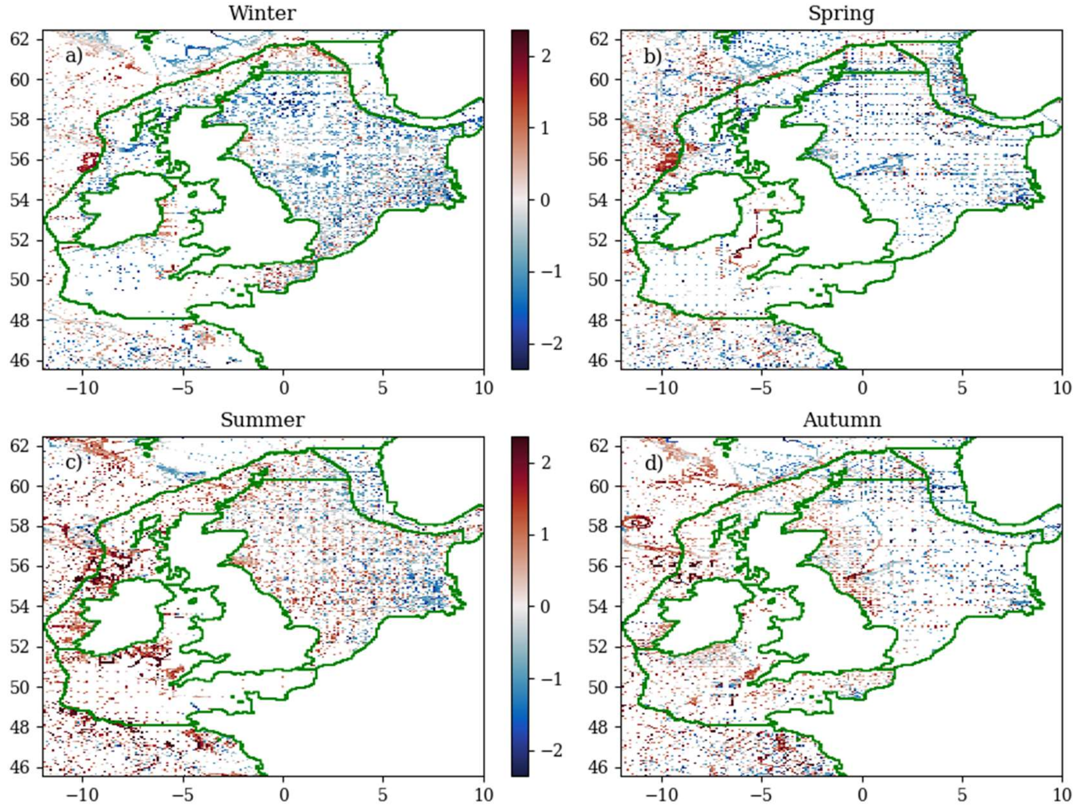

Figure S4 Model-EN4 SST biases normalised by the ensemble standard deviation for the four season (a-d) – effectively the number of ensemble standard deviations the observations are from the ensemble mean. See text for details.

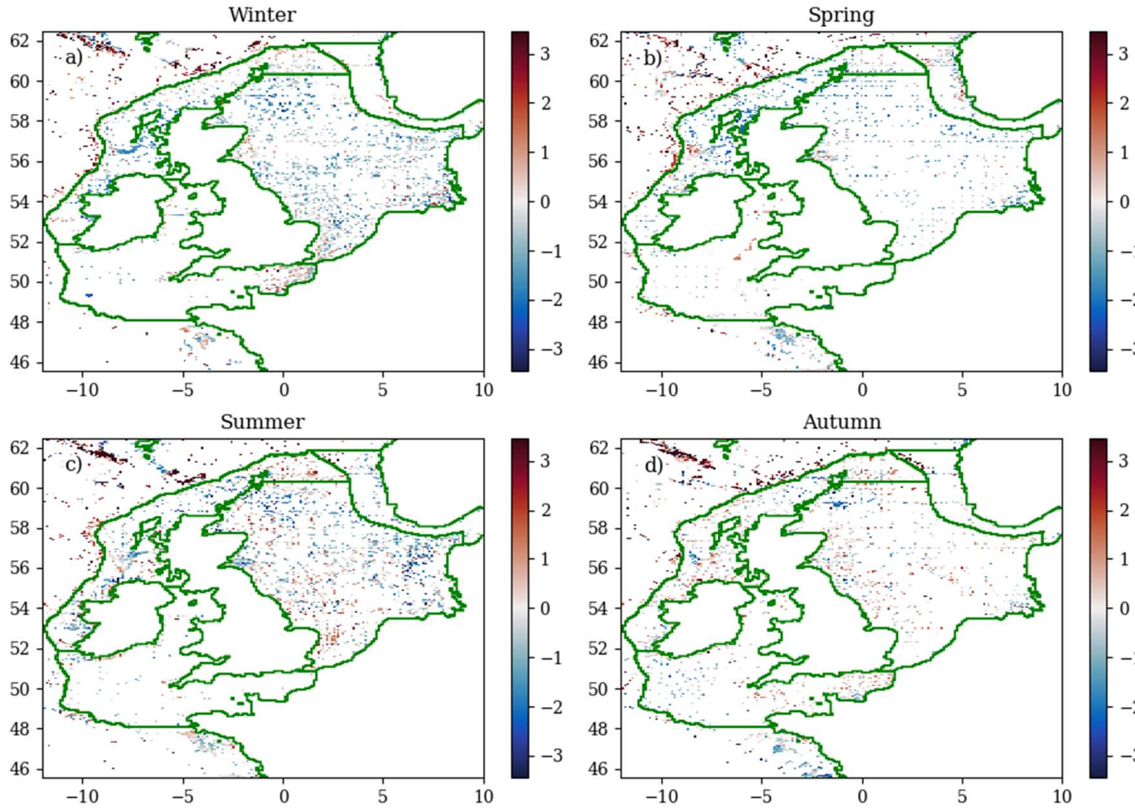

Figure S5 as Model-EN4 NBT biases normalised by the ensemble standard deviation for the four season (a-d) – effectively the number of ensemble standard deviations the observations are from the ensemble mean. See text for details.

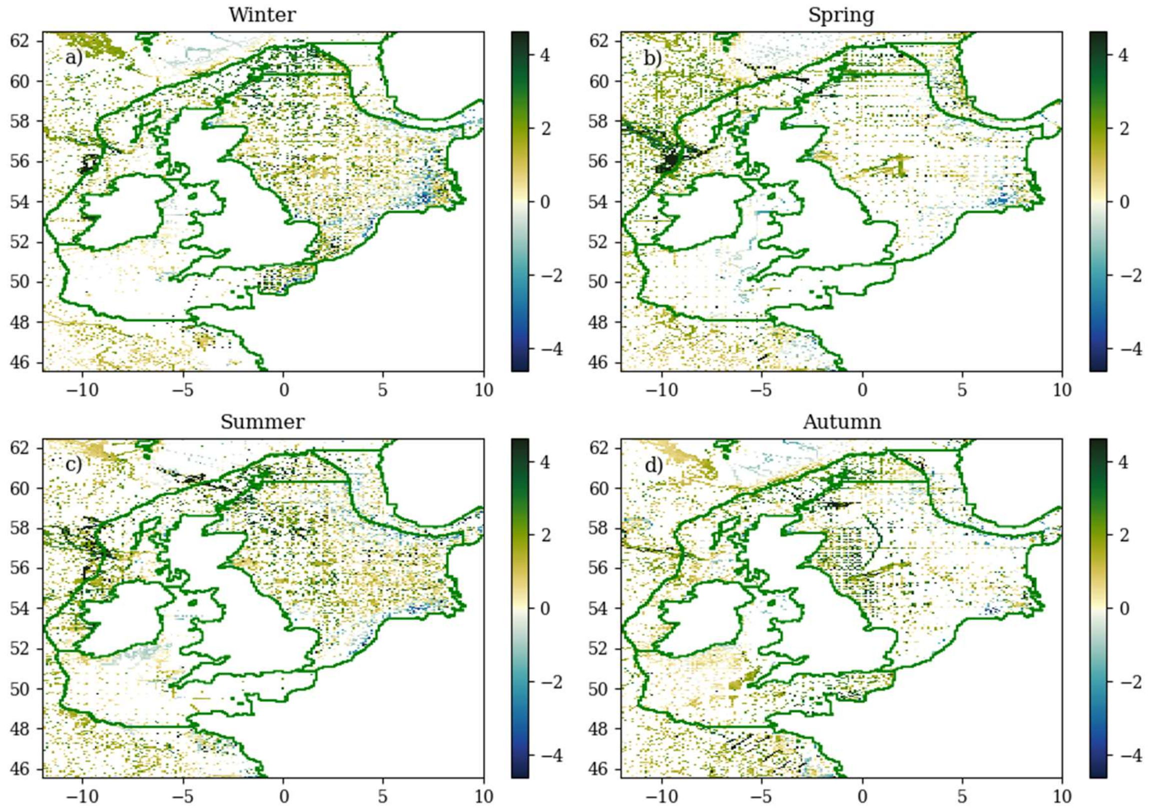

Figure S6 as Model-EN4 SSS biases normalised by the ensemble standard deviation for the four season (a-d) – effectively the number of ensemble standard deviations the observations are from the ensemble mean. See text for details.

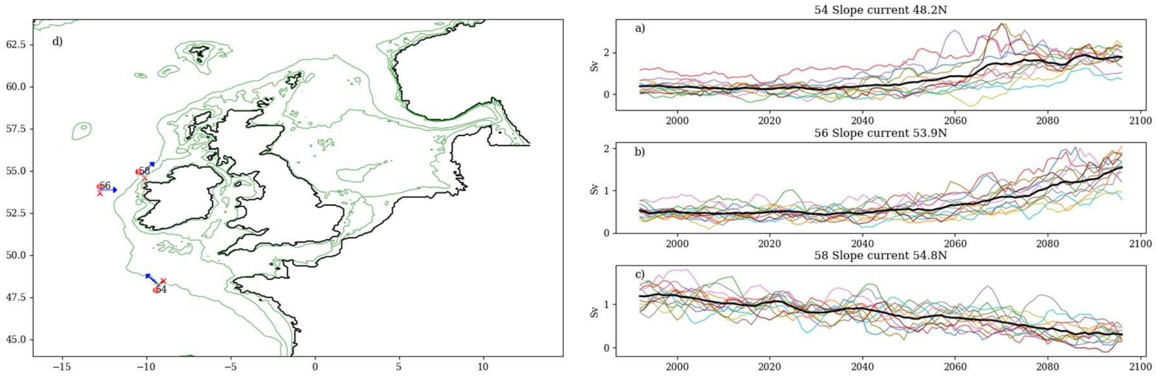

Figure S7 Net volume transport through cross-sections. a-c: time series of the annual mean net transport (Sv) for all 12 ensemble members of the NWSPPE (with a 5-year running mean), and the ensemble mean (black line). The locations of the cross-sections are given in d, and in Table S2.

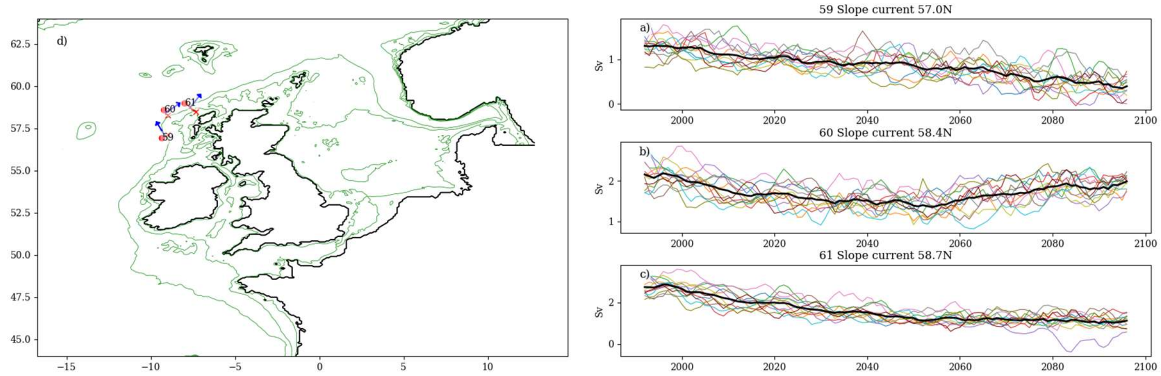

Figure S8 Net volume transport through cross-sections. a-c: time series of the annual mean net transport (Sv) for all 12 ensemble members of the NWSPPE (with a 5-year running mean), and the ensemble mean (black line). The locations of the cross-sections are given in d, and in Table S2.

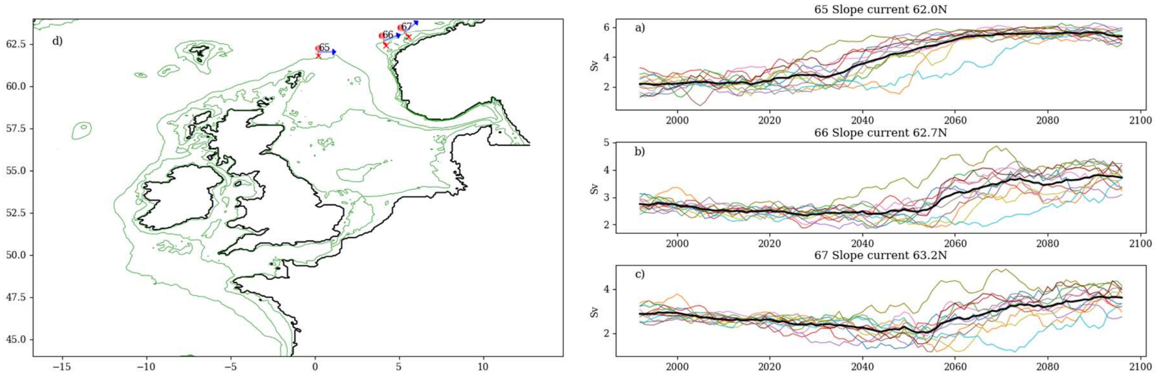

Figure S9 Net volume transport through cross-sections. a-c: time series of the annual mean net transport (Sv) for all 12 ensemble members of the NWSPPE (with a 5-year running mean), and the ensemble mean (black line). The locations of the cross-sections are given in d, and in Table S2.

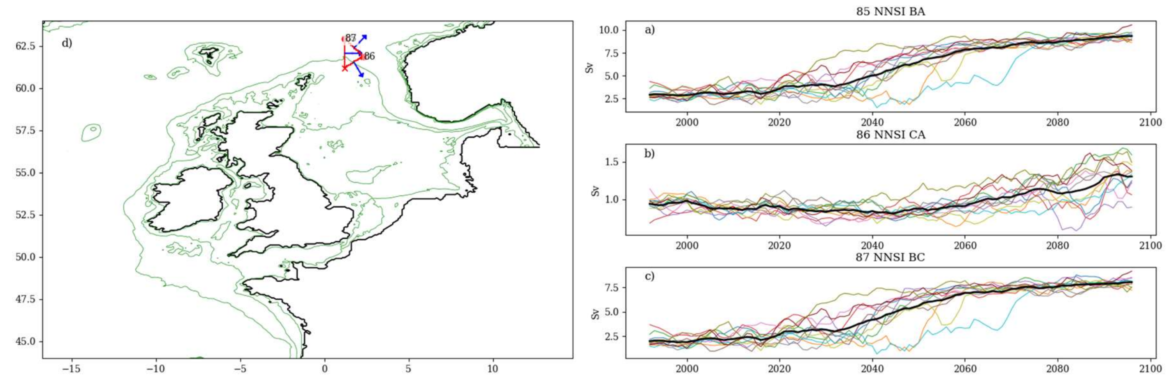

Figure S10 Net volume transport through cross-sections. a-c: time series of the annual mean net transport (Sv) for all 12 ensemble members of the NWSPPE (with a 5-year running mean), and the ensemble mean (black line). The locations of the cross-sections are given in d, and in Table S2.

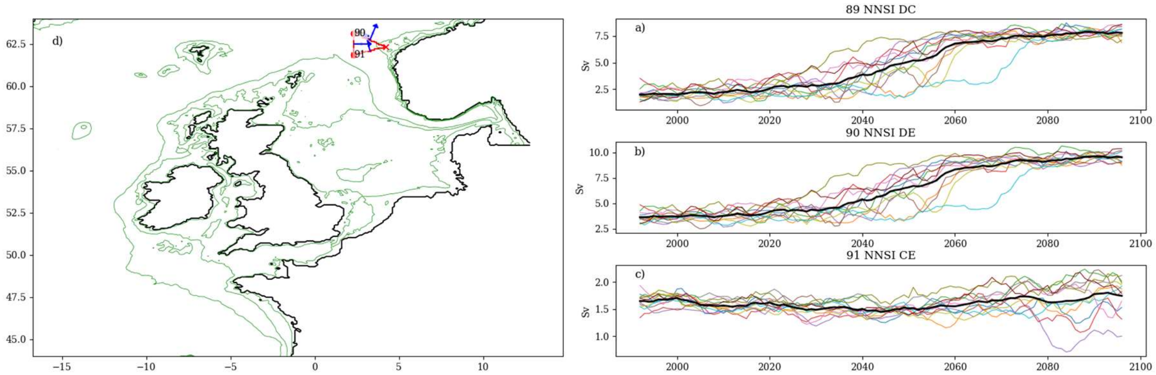

Figure S11 Net volume transport through cross-sections. a-c: time series of the annual mean net transport (Sv) for all 12 ensemble members of the NWSPPE (with a 5-year running mean), and the ensemble mean (black line). The locations of the cross-sections are given in d, and in Table S2.

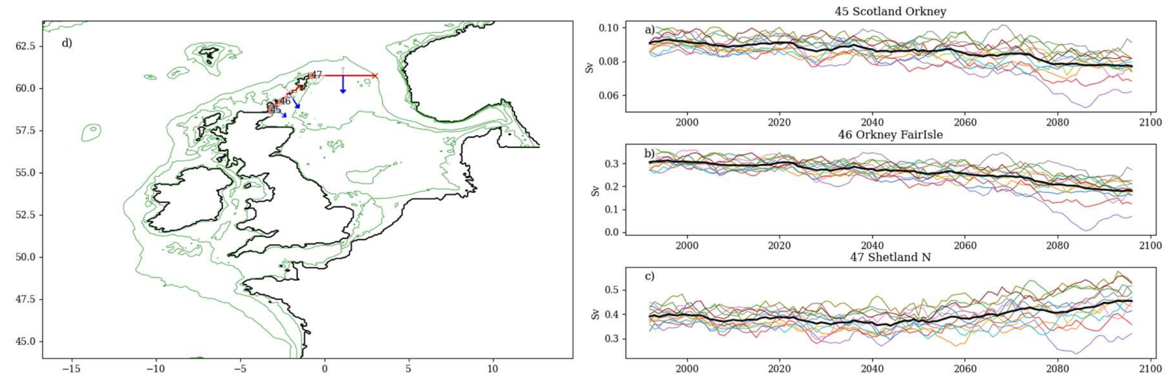

Figure S12 Net volume transport through cross-sections. a-c: time series of the annual mean net transport (Sv) for all 12 ensemble members of the NWSPPE (with a 5-year running mean), and the ensemble mean (black line). The locations of the cross-sections are given in d, and in Table S2.

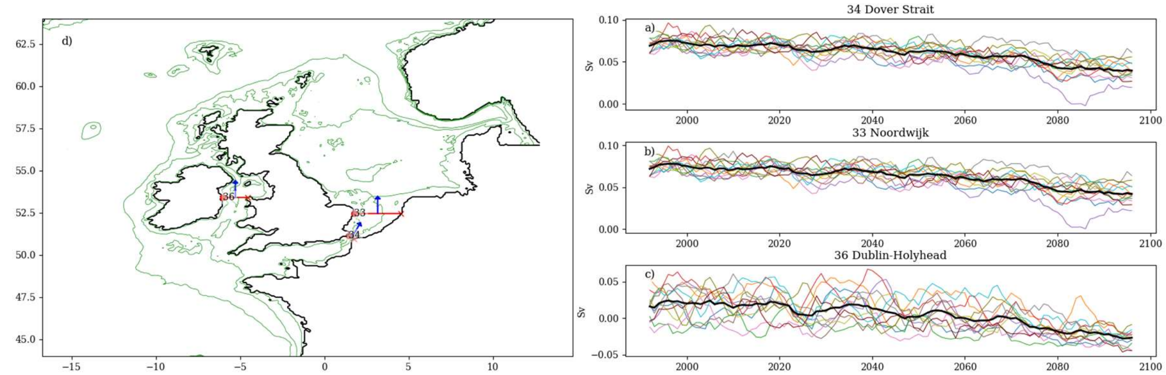

Figure S13 Net volume transport through cross-sections. a-c: time series of the annual mean net transport (Sv) for all 12 ensemble members of the NWSPPE (with a 5-year running mean), and the ensemble mean (black line). The locations of the cross-sections are given in d, and in Table S2.

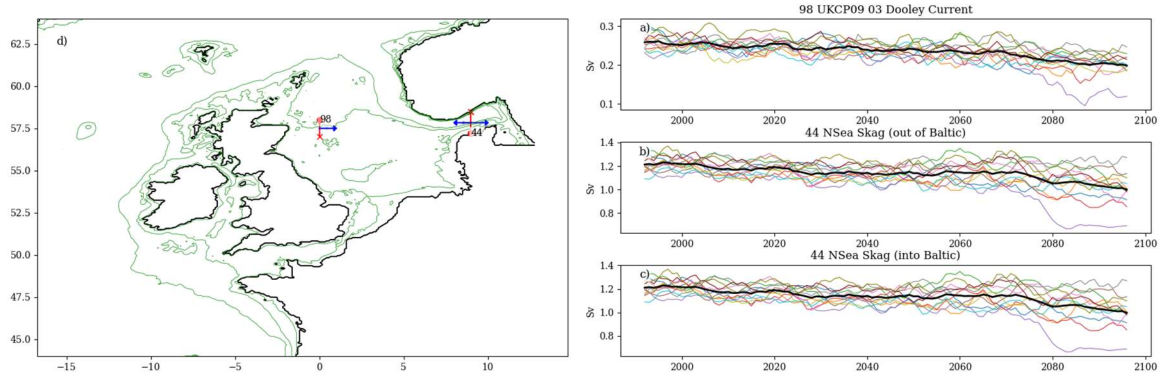

Figure S14 Net volume transport through cross-sections. a-c: time series of the annual mean net transport (Sv) for all 12 ensemble members of the NWSPPE (with a 5-year running mean), and the ensemble mean (black line). b and c present the positive and negative components of the Baltic outflow, rather than the net transport. The locations of the cross-sections are given in d, and in Table S2.

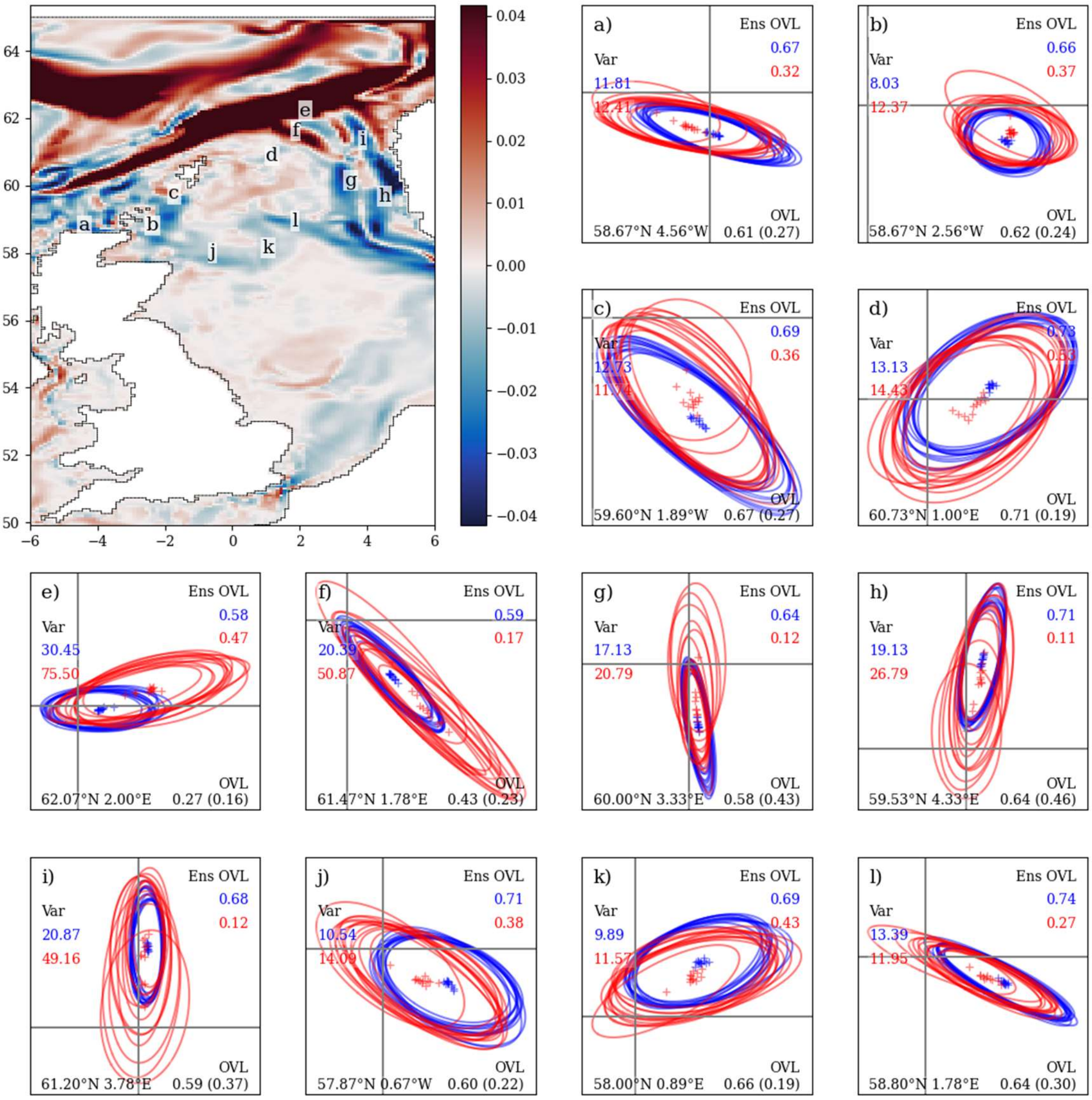

Figure S15 Point examples of the residual current uncertainty ellipses in the Northern North Sea. a-l: early and late 21st Century (2000-2019: blue; 2079-2098: red) mean residual transport for all 12 ensemble members are given as colours crosses. Due to the variability, the residual current will not always equal the long term mean and will vary in terms of strength and direction. Using the current uncertainty ellipses approach of Tinker et al. (2022), we can fit a bivariate normal distribution, and delineate where the residual current is likely to be for a given percentage of the time - this is shown in the coloured ellipses (one for each ensemble member). We can then use this approach to compare the variability of the distributions, how much overlap there is between the distributions across the ensemble in the early and late 21st Century, and how much the overlap changes between early and late 21st Century for each ensemble member (the ensemble mean, and ensemble standard deviation in brackets) – these are reported in the upper left, upper right, and lower right for each sub-panel. The exemplar locations are given on the map in the main upper right panel, and as longitude and latitudes in the lower left of each sub-panel.

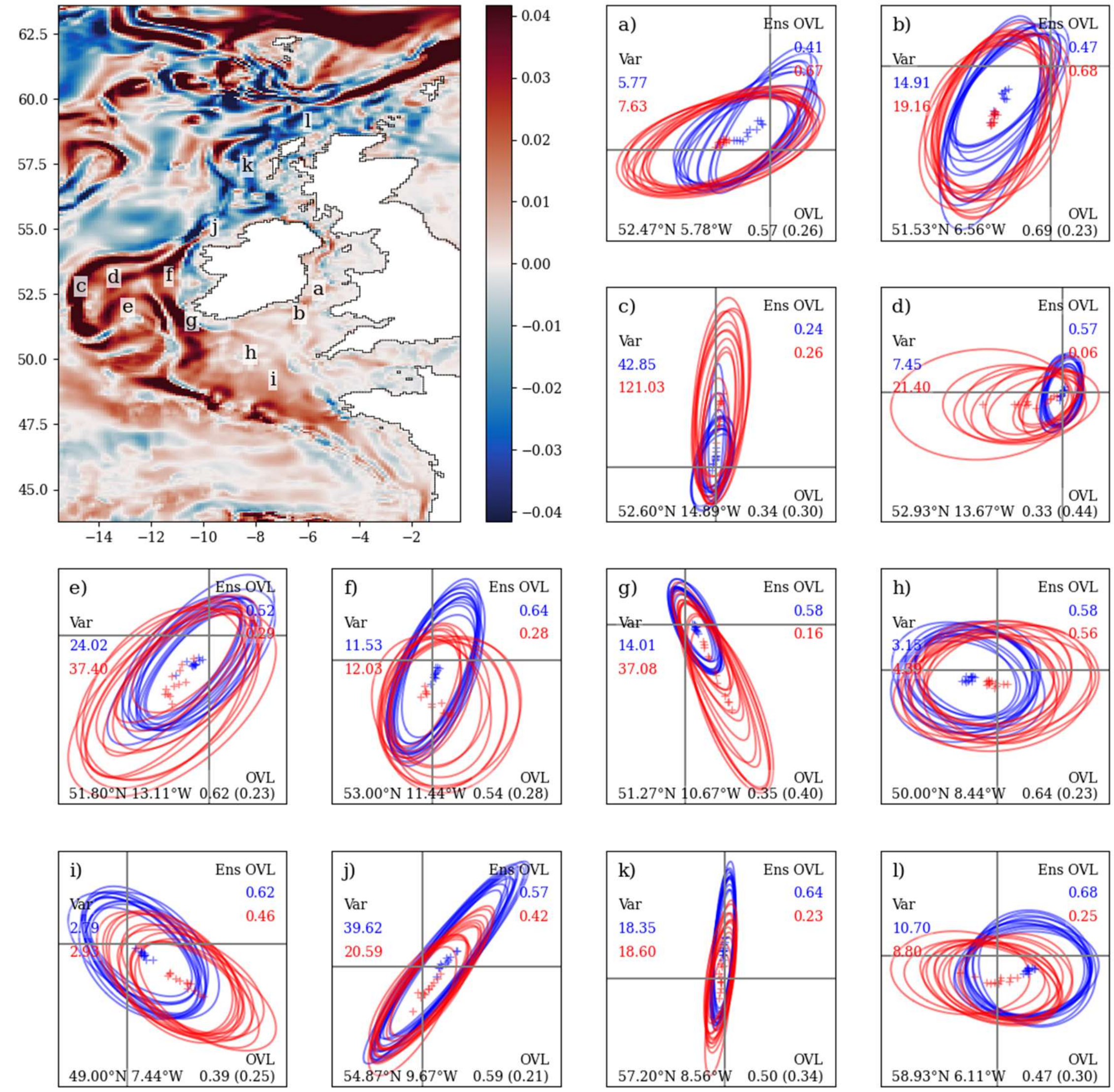

Figure S16 Point examples of the residual current uncertainty ellipses in the Southwest Approaches. a-l: early and late 21st Century (2000-2019: blue; 2079-2098: red) mean residual transport for all 12 ensemble members are given as colours crosses. Due to the variability, the residual current will not always equal the long term mean and will vary in terms of strength and direction. Using the current uncertainty ellipses approach of Tinker et al. (2022), we can fit a bivariate normal distribution, and delineate where the residual current is likely to be for a given percentage of the time - this is shown in the coloured ellipses (one for each ensemble member). We can then use this approach to compare the variability of the distributions, how much overlap there is between the distributions across the ensemble in the early and late 21st Century, and how much the overlap changes between early and late 21st Century for each ensemble member (the ensemble mean, and ensemble standard deviation in brackets) – these are reported in the upper left, upper right, and lower right for each sub-panel. The exemplar locations are given on the map in the main upper right panel, and as longitude and latitudes in the lower left of each sub-panel.

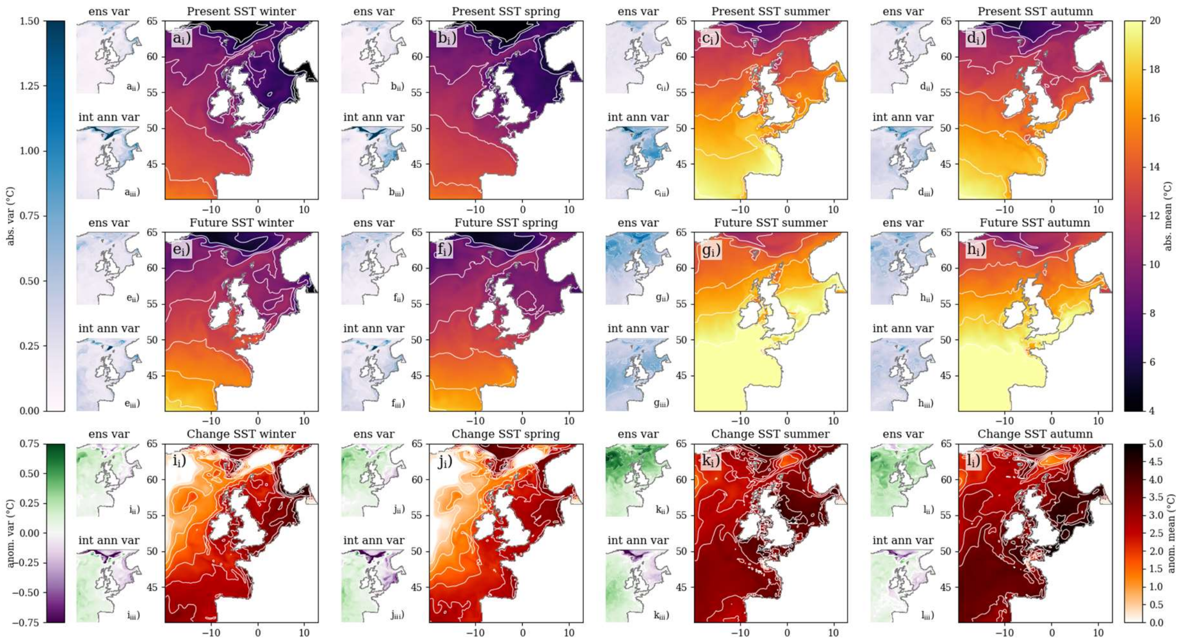

Figure S17 The early-century (2000-2019, upper row, a-d) and late-century (2079-2098, middle row, e-h) SST and their difference (bottom row, i-l). The four main columns give the seasons (winter: December-February (a, e, i); spring March-May (b, f, j); summer June- August (c, g, k); autumn September- November (d, h, l)). For each column and row, the main panel gives the ensemble mean ($_{i}$), while the smaller panels on the left give the ensemble and interannual variability (upper ($_{ii}$) and lower row ($_{iii}$) respectrively).

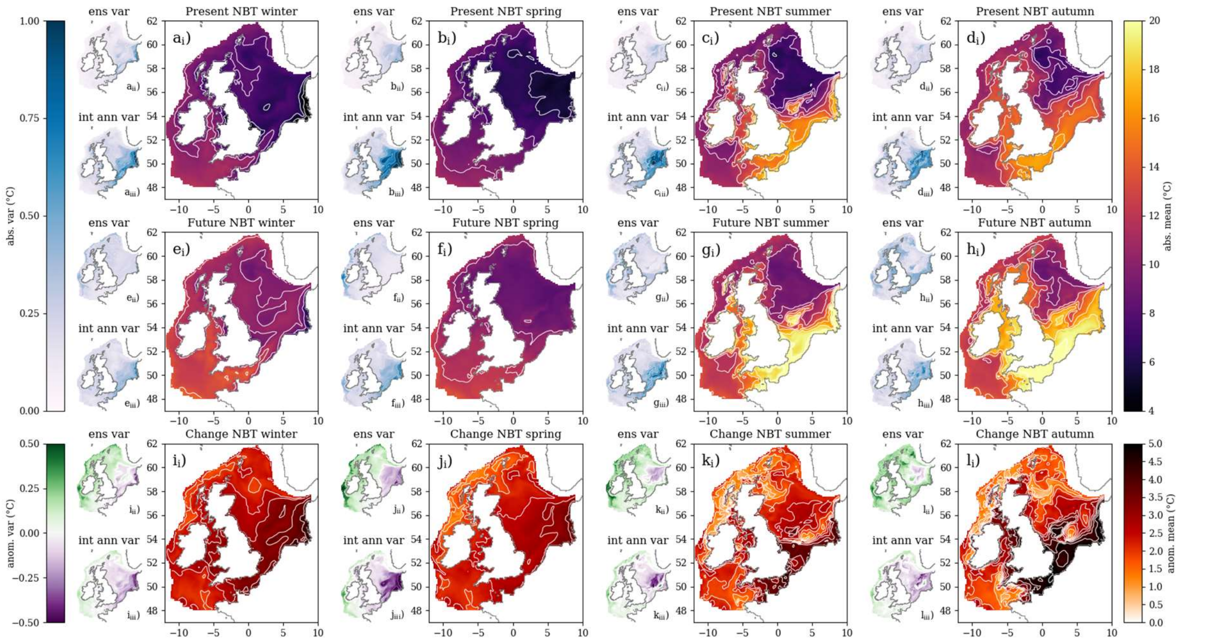

Figure S18 The early-century (2000-2019, upper row, a-d) and late-century (2079-2098, middle row, e-h) NBT and their difference (bottom row, i-l). The four main columns give the seasons (winter: December-February (a, e, i); spring March-May (b, f, j); summer June- August (c, g, k); autumn September- November (d, h, l)). For each column and row, the main panel gives the ensemble mean ($_{i}$), while the smaller panels on the left give the ensemble and interannual variability (upper ($_{ii}$) and lower row ($_{iii}$) respectively).

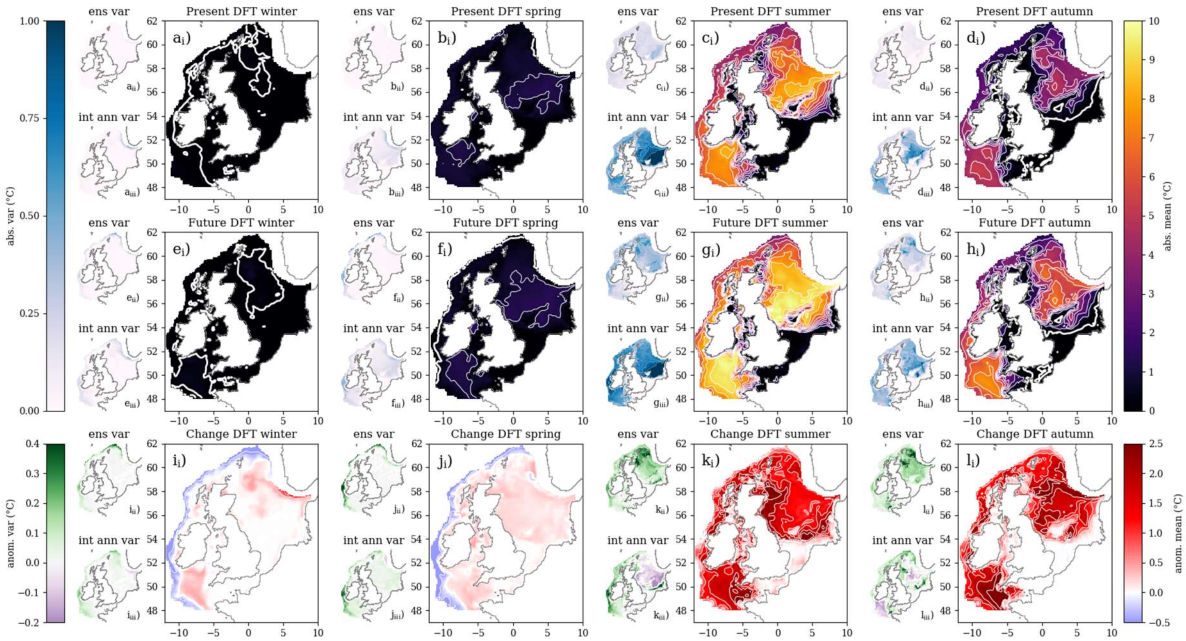

Figure S19 The early-century (2000-2019, upper row, a-d) and late-century (2079-2098, middle row, e-h) DFT and their difference (bottom row, i-l). The four main columns give the seasons (winter: December-February (a, e, i); spring March-May (b, f, j); summer June- August (c, g, k); autumn September- November (d, h, l)). For each column and row, the main panel gives the ensemble mean ($_{i}$), while the smaller panels on the left give the ensemble and interannual variability (upper ($_{ii}$) and lower row ($_{iii}$) respectrively).

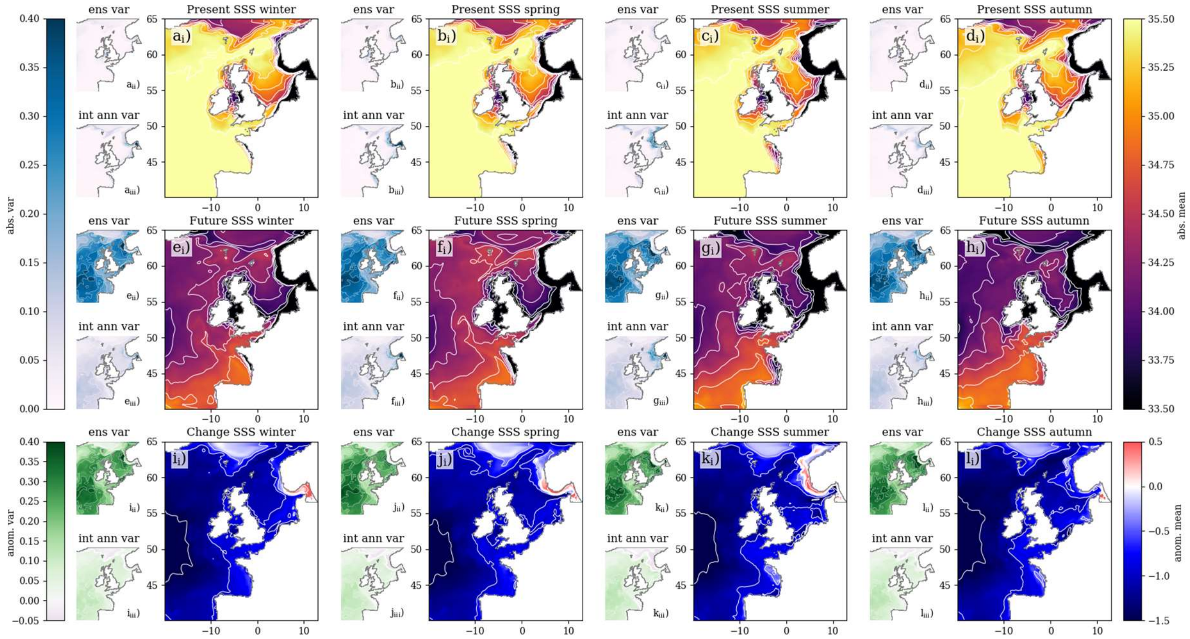

Figure S20 The early-century (2000-2019, upper row, a-d) and late-century (2079-2098, middle row, e-h) SSS and their difference (bottom row, i-l). The four main columns give the seasons (winter: December-February (a, e, i); spring March-May (b, f, j); summer June- August (c, g, k); autumn September- November (d, h, l)). For each column and row, the main panel gives the ensemble mean ($_i$), while the smaller panels on the left give the ensemble and interannual variability (upper ($_{ii}$) and lower row ($_{iii}$) respectively).

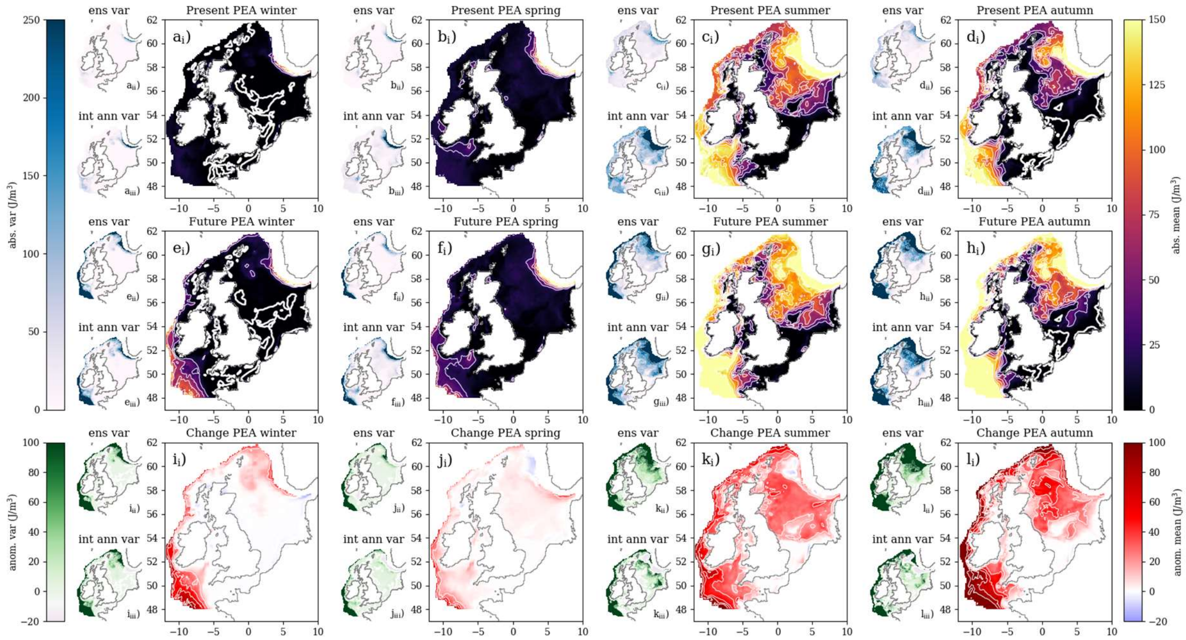

Figure S21 The early-century (2000-2019, upper row, a-d) and late-century (2079-2098, middle row, e-h) PEA and their difference (bottom row, i-l). The four main columns give the seasons (winter: December-February (a, e, i); spring March-May (b, f, j); summer June- August (c, g, k); autumn September- November (d, h, l)). For each column and row, the main panel gives the ensemble mean ($_{i}$), while the smaller panels on the left give the ensemble and interannual variability (upper ($_{ii}$) and lower row ($_{iii}$) respectrively).

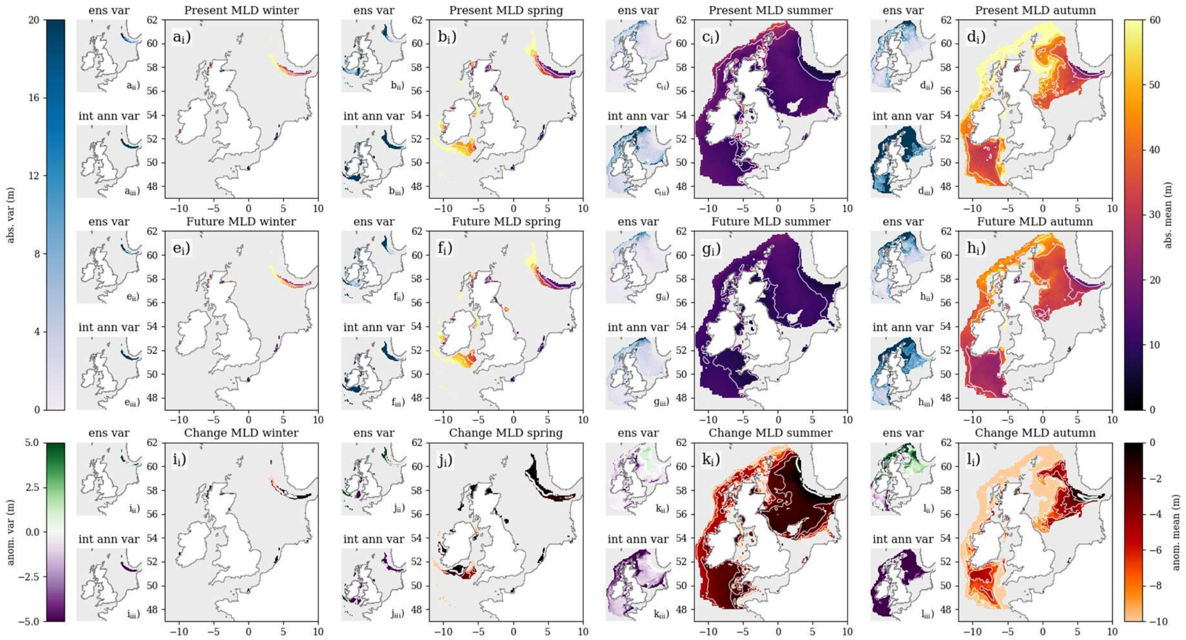

Figure S22 The early-century (2000-2019, upper row, a-d) and late-century (2079-2098, middle row, e-h) MLD and their difference (bottom row, i-l). The four main columns give the seasons (winter: December-February (a, e, i); spring March-May (b, f, j); summer June- August (c, g, k); autumn September- November (d, h, l)). For each column and row, the main panel gives the ensemble mean ($_i$), while the smaller panels on the left give the ensemble and interannual variability (upper ($_{ii}$) and lower row ($_{iii}$) respectrively).

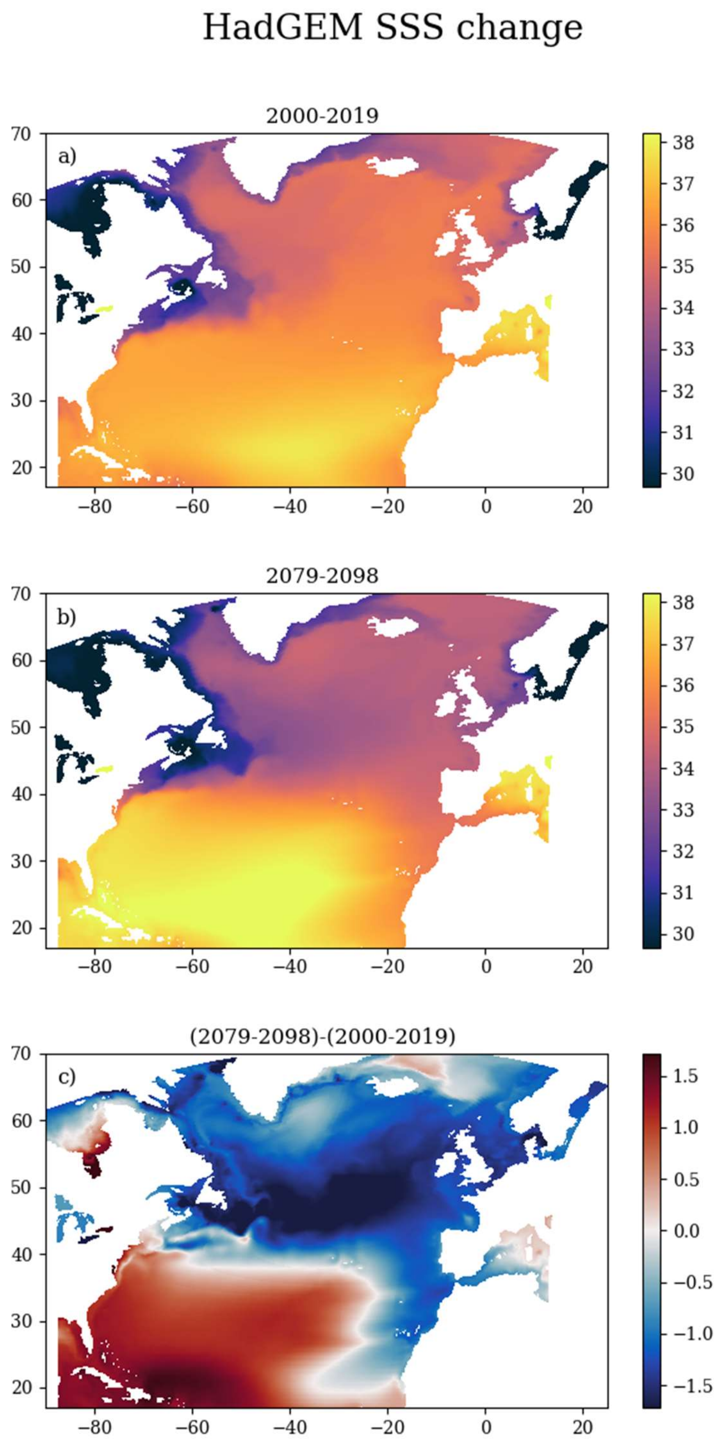

Figure S23 HadGEM3 GC3.05 ensemble mean SSS, for a) early 21st century (2000-2019); b) late 21st century (2079-2098), and; c) the difference (2079-2098 minus 2000-2019). Salinities are given on the (unitless) practical salinity scale.

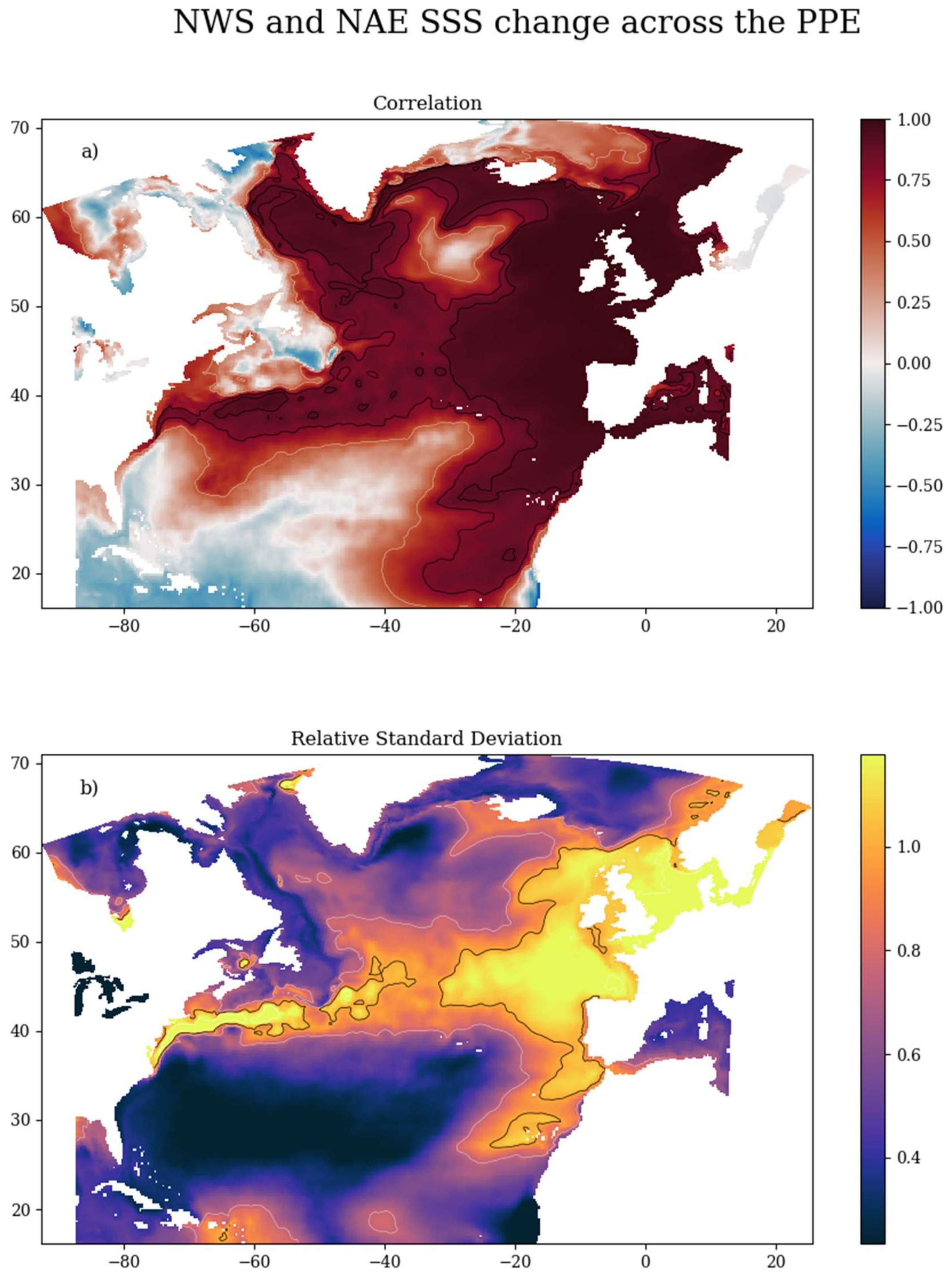

Figure S24 – a) Ensemble correlation, and b) relative standard deviation between NWS regional mean SSS change (2079-2098 – 2000-2019) and pointwise HadGEM3 SSS change. The contours represent a) white: 0.532, where p>0.05 for n = 12 (ensemble members); black 0.9 and 0.8; b) black = 1; white = 0.75 and 1.25.

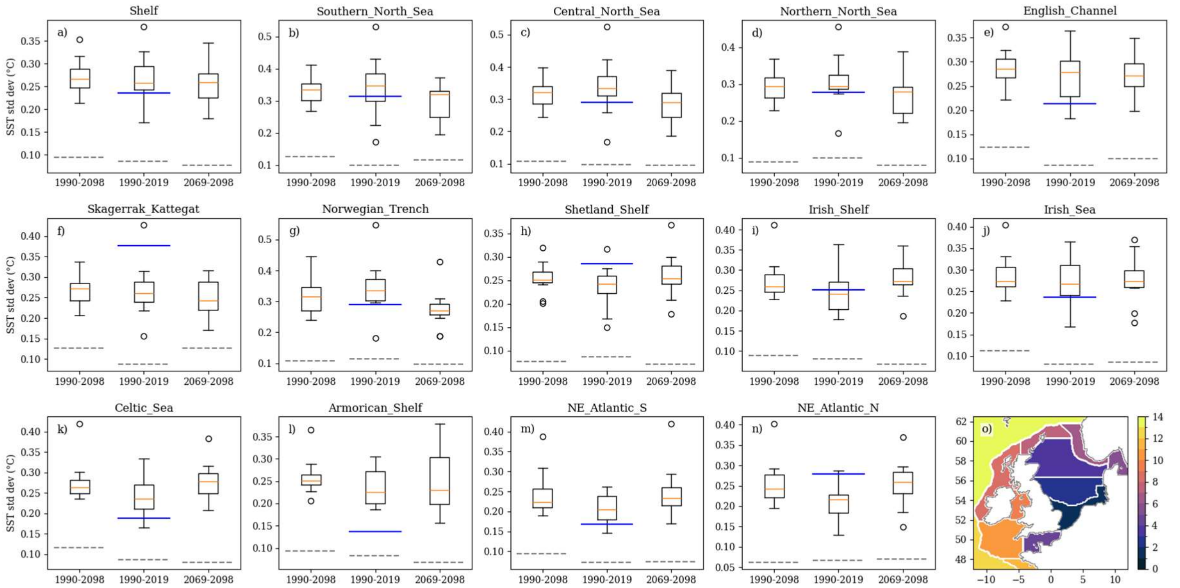

Figure S25 SST (de-seasonalised and detrended) low frequency (<5 yr) interannual variability for 1990-2098, 1990-2019 and 2069-2098. Each ensemble member annual mean time series is filtered with a 5-year low pass filter. The standard deviation is then calculated for the appropriate time-period, giving a distribution of 12 interannual variability estimates for the NWSPPE. These distributions are then plotted as box and whisker plots. The same method is applied to the NWSPPE ensemble mean, and the RAN (only for the 1990-2019 period), which are plotted as dotted grey and blue lines respectively. a-n) the NWS regions, and o) the NWS region mask.

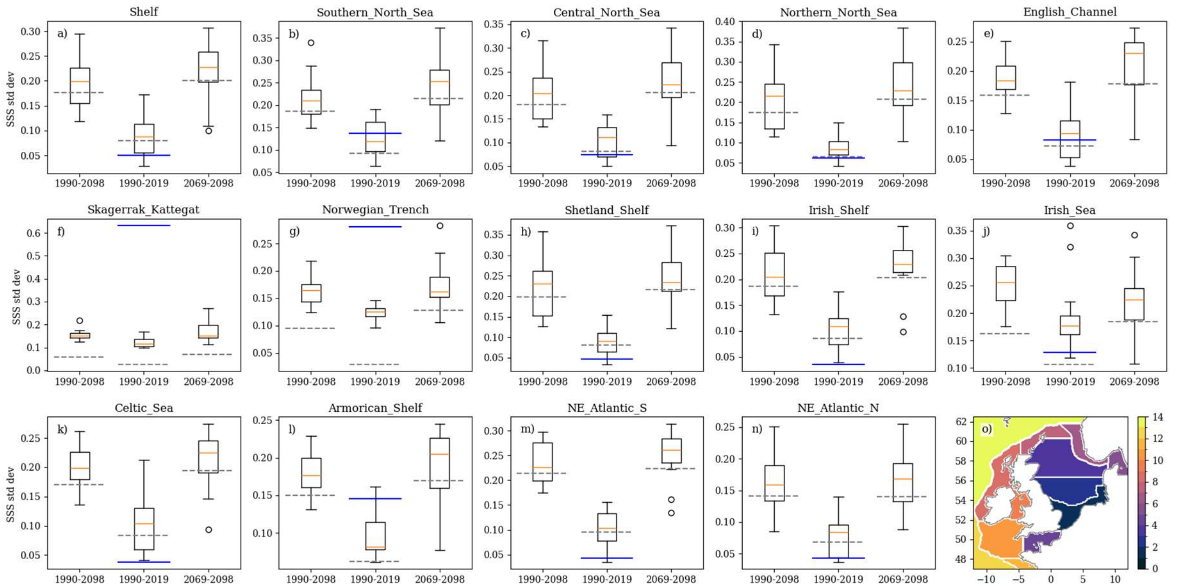

Figure S26 SSS (de-seasonalised and detrended) low frequency (<5 yr) interannual variability for 1990-2098, 1990-2019 and 2069-2098. Each ensemble member annual mean time series is filtered with a 5-year low pass filter. The standard deviation is then calculated for the appropriate time-period, giving a distribution of 12 interannual variability estimates for the NWSPPE. These distributions are then plotted as box and whisker plots. The same method is applied to the NWSPPE ensemble mean, and the RAN (only for the 1990-2019 period), which are plotted as dotted grey and blue lines respectively. a-n) the NWS regions, and o) the NWS region mask. Salinities are given on the (unitless) practical salinity scale.

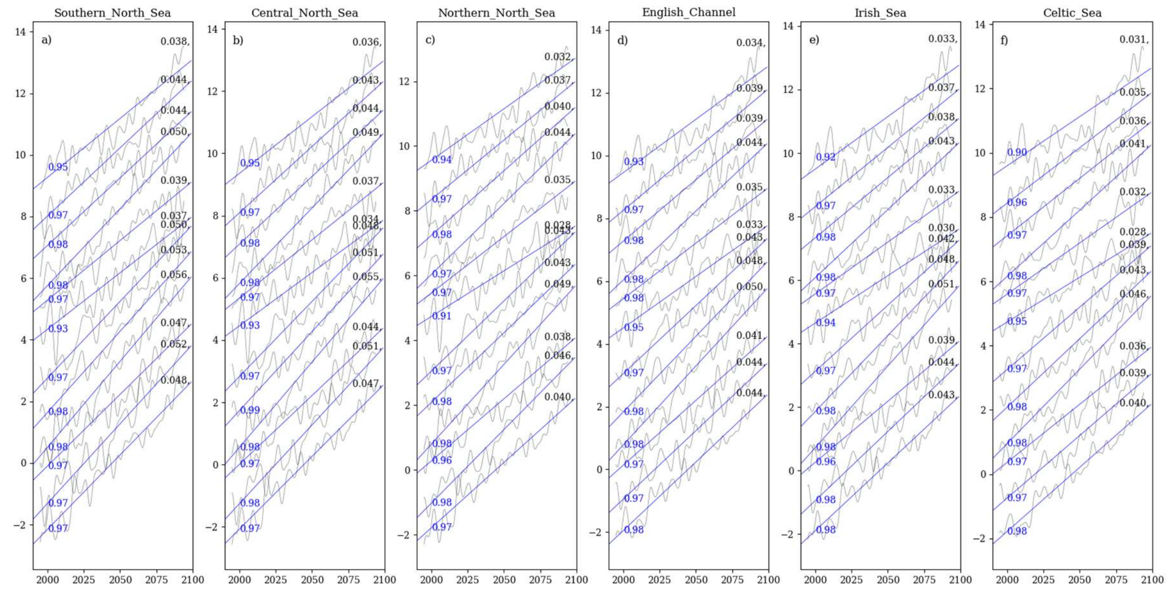

Figure S27 Linear fits for (de-seasonalised) SST trends for each ensemble member (each line is offset) for selected inner shelf regions (a-f – see region mask in Figure 14). On the left of each line is the correlation of the fit (blue), and the right is the gradient (black).

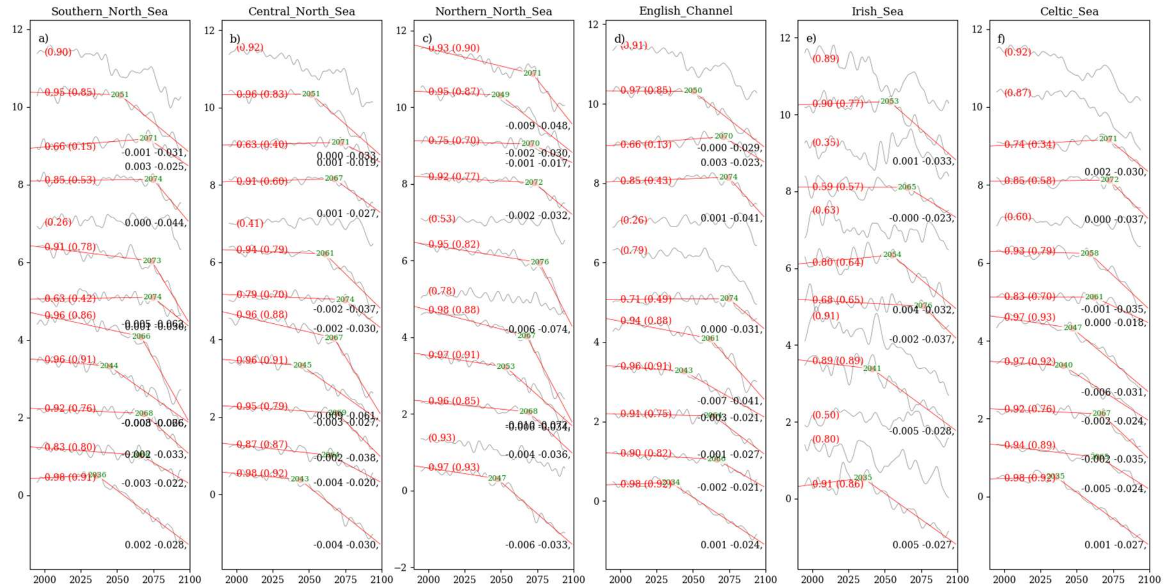

Figure S28 Based on Figure S27 for (de-seasonalised) SSS, but rather than a single linear fit, two intersecting lines are fitted with a curve fitting program. Where the correlation is improved (compared with a single line), it is plotted in red. The correlation is given in red (and for the single linear fit in brackets). The slope of the first and second line is given in black. The year where the slope changes is given in green.

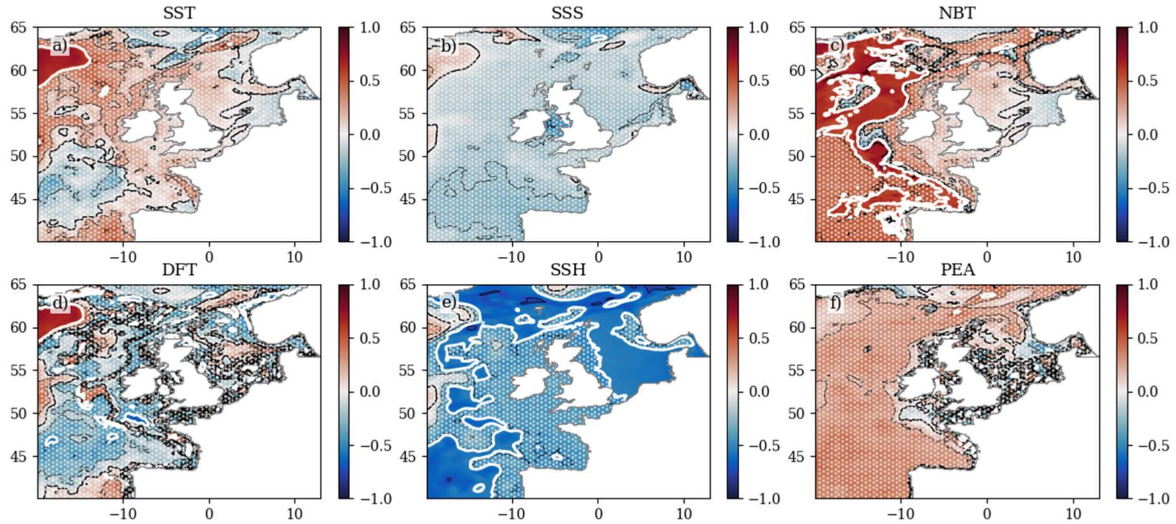

Figure S29 Correlation between NWS winter change, and AMOC (at 26°N) change, both the difference between the 2069-2098 and 1990-2019 mean. a) Winter (DJF) SST change (2069-2098 mean minus 1990-2019 mean) for each of the 12 NWSPPE ensemble members is correlated against the (annual mean) AMOC slow down (between the same periods) on a point-by-point basis. This is repeated for b) SSS; c) NBT; d) DFT; e) SSH and f) PEA. The (annual mean) AMOC slowdown is given in Table S9.

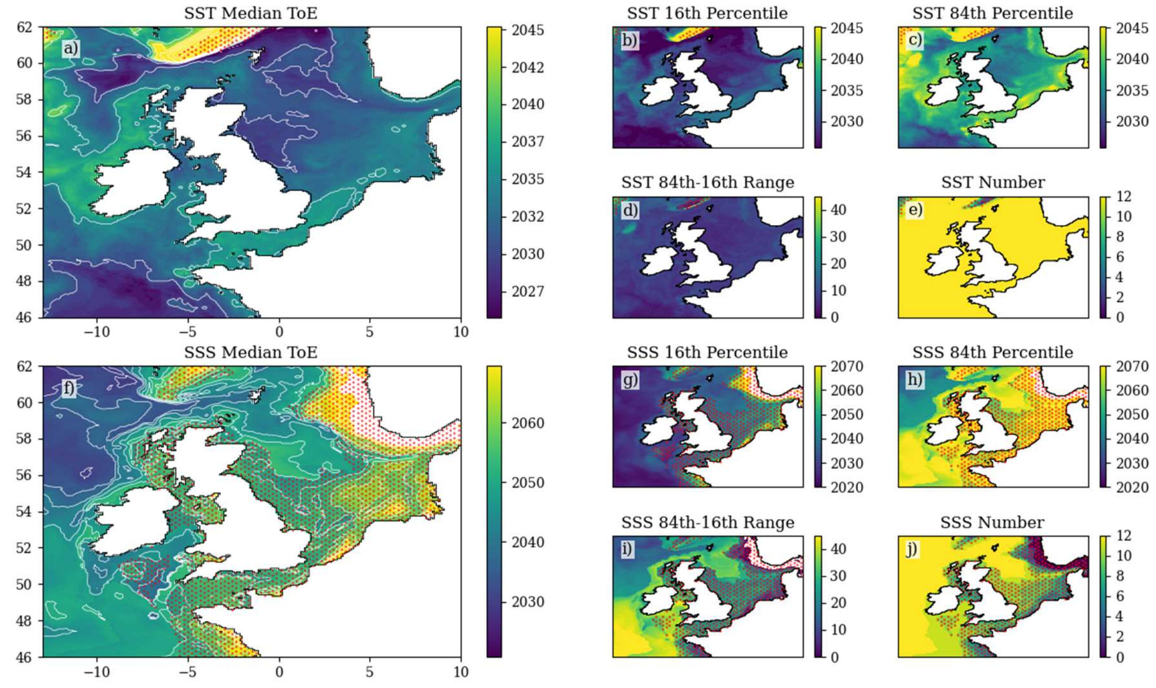

Figure S30 Estimates of the Time of Emergence for SST (a-e) and SSS (f-j) following the Lyu et al., (2014) method. ToE is calculated for each ensemble member of the NWSPPE, and the median range is given in a) and f) with the 16th (b, g) and 84th (c, h) percentile value, and their (16th-84th percentile) range (e, j). The number of ensemble members where the climate signal emerges is given in e) and j). Stippling shows where less than 84% of the ensemble (10 out of 12 members) show emergence.